

## Numerical Modelling of Caseless Ammunition with Coreless Bullet in Internal Ballistics

U.S. Silva Rivera<sup>1</sup>, J.M. Sandoval Pineda<sup>#,\*</sup>, O. Susarrey-Huerta<sup>1</sup>,  
L.A. Flores Herrera<sup>#</sup>, and P.A. Tamayo Meza<sup>#</sup>

<sup>1</sup>*Instituto Politécnico Nacional, ESIME-SEPI, U. Zacatenco, 07738, México*  
<sup>#</sup>*Instituto Politécnico Nacional, ESIME-SEPI, U. Azcapotzalco, 02250, México*  
<sup>\*</sup>*E-mail: jsandovalp@ipn.mx*

### ABSTRACT

In the search of a new weapon for combat in short range, it is proposed the use of a new experimentally designed 7.62 mm calibre ammunition with a lighter weight (caseless-coreless). This can be used in carbine assault rifles with short barrel or pistols. In this work, the compressible gases flowing through the gun barrel caused by the proposed ammunition were experimentally and numerically analysed. The Large Eddy Simulation was used for the numerical simulation, considering a compressible and turbulent flow, with the chemical species transport model and a complete conversion of the propellant reaction. Variations in pressure and temperature were compared with the results obtained from a conventional 7.62 mm full metal jacket (FMJ) ammunition. Results of ballistic experimental tests and numerical simulations were similar than those of the 9 mm x 19 mm FMJ ammunitions, showing feasibility for the development of new weapons intended for operations of short range shots.

**Keywords:** Compressible flow, deflagration, Eddy-dissipation model, caseless-coreless

### NOMENCLATURE

$A$	Empirical constant equal to 4
$B$	Empirical constant equal to 0.5
$i$	Net rate of production of species due to the $r$ reaction
$P$	Static pressure
$T$	Absolute temperature
$V$	Velocity
$Y_p$	Mass fraction of any product species $P$
$Y_R$	Mass fraction of a particular $R$ reactant

### 1. INTRODUCTION

Analysis of gas flow occurs within a gun is a complex problem that is studied from several aspects and can be related to some conditions that happen in combustion chambers or in vessels under high pressure. Common analyses are focused on the reaction of the propellants or fuels<sup>1-3</sup>, and the pressure gradient generated by conventional projectiles and in high-pressure vessels<sup>4-6</sup>. These studies consider the gases produced by the ignition or combustion of the propellant as a compressible turbulent flow solved with computational fluid dynamics (CFD) by several turbulence modelling approaches such as the Eulerian-Lagrange<sup>7</sup>, the Reynolds-Averaged Navier-Stokes (RANS) equations<sup>8,9</sup>, Direct numerical simulation (DNS)<sup>10-12</sup>, or with large Eddy simulation (LES)<sup>13-16</sup>. DNS is currently the most accurate method, but it is also the most computationally-expensive, because it requires that all of the significant turbulent structures are properly captured. In some cases, the LES has better results, it directly solves the large-scale motion and approximates the motion in small scale<sup>17</sup>. There are also studies

of caseless ammunition, combustible case and binders<sup>18-20</sup>, these ammunitions and their weapons allow a higher volume of fire-increasing benefits during combat conditions and saving metal cases. It is known that some studies suggest that the use of propellants of nitrocellulose are not the most appropriate for caseless ammunition and combustible cartridge cases, because these are more sensitive to friction and heat<sup>19</sup>.

In this study, a new 7.62 mm caseless ammunition with coreless bullet (caseless-coreless) is presented, being the aim of this work to determine whether the generated ballistic parameters are equivalent to the 9 mm x 19 mm FMJ ammunition, to have application in the development of weapons to be used by the enforcement of the law in urban operations or short range shots. This represents a new physical phenomenon, because the behaviour of the gas flow introduced inside the bullet without core is still not well known in interior ballistics. The numerical study of the new 7.62 mm caseless-coreless ammunition was corroborated with experimental tests carried out on manufactured prototypes and compared with standardised experimental tests<sup>21</sup>.

### 2. PROCEDURE

#### 2.1 Species Transport

The Eddy-dissipation model was used for the internal ballistic simulation<sup>16</sup>. It was considered a turbulent flow regime including the chemical species transport, the mixing of double-base gunpowder, a complete conversion of the reaction and a pressure-based solver for the combustion simulation<sup>17</sup>. The turbulence-chemistry interaction model can be expressed by

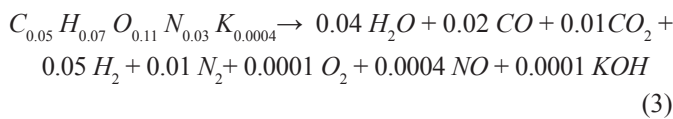
Eqns (1) and (2)<sup>22</sup>:

$$R_{i,r} = v'_{i,r} M_{w,i} A \rho \frac{\varepsilon}{k} \min R \frac{Y_R}{v'_{R,r} M_{w,R}} \quad (1)$$

$$R_{i,r} = v'_{i,r} M_{w,i} A B \rho \frac{\varepsilon}{k} \frac{\sum_P Y_P}{\sum_j v'_{j,r} M_{w,j}} \quad (2)$$

where  $i$ , is the net rate of production of species due to the  $r$  reaction;  $R_{i,r}$  is given by the smaller limiting value of the Eqns (1) and (2);  $Y_p$  is the mass fraction of any product species  $P$ ;  $Y_R$  is the mass fraction of a particular  $R$  reactant;  $A$  is an empirical constant equal to 4, and  $B$  is an empirical constant equal to 0.5.

To have a reduced number of variables that could affect the comparison of results, the same double-base gunpowder was used in the 7.62 x 51 mm FMJ ammunition and in the 7.62 mm caseless-coreless ammunition, performing calculations with the same specifications of chemical composition, density, heat capacity, and enthalpy. The calculation of the chemical reaction was carried out with the ICT-Thermodynamic-Code<sup>®</sup>, and the main chemical species studied were nitrocellulose (13.25 per cent  $N$ ), nitroglycerin, potassium nitrate, centralite  $I$  and ethanol, excluding insignificant gaseous products. The reaction for 2.90 g of double base gunpowder is shown in Eqn (3):



### 2.2 Numerical Analysis

The volume of gases generated by the new 7.62 mm caseless ammunition with coreless bullet in the test barrel was analysed in a set of 10 progressive steady systems. During the simulations, the length of the chamber remained constant, but the model was gradually increased by changing the position of the jacket and extending the length of the barrel from 3 mm up to its final length of 446 mm, using 8 increments of 50 mm each one and the last one of 43 mm. Additional data was also included like the density of double-base gunpowder which was

considered of 210 kg/m<sup>3</sup>, the specific heat ratio of 1.2105, the maximum pressure of 400 MPa, and a stagnation temperature of 3200 °K.

Figure 1(a) shows a longitudinal slice of the 3-D caseless-coreless ammunition model in the hermetic chamber. In this case, the primer is inserted on the rear side of the agglutinated powder and the coreless bullet is filled with the combustion gases. Figure 1(b) shows a close view of the resulting meshing in the contact zone between the jacket of the coreless bullet and the barrel grooves. This is quite significant because it represents the system at the time of shooting; just at 0.002 ms when the powder gases have reached the piezoelectric transducer.

A numerical simulation for the 7.62 mm x 51 mm FMJ ammunition was performed, to validate the proposed numerical system. Figure 2(a) shows the second case of modelling with a conventional ammunition. This corresponds to the moment when the deflagration of the gunpowder was initiated, and the gases reach the piezoelectric transducer slot located at 53 mm from the rear side of the barrel. Figure 2(b) shows the quality of the cut-cell mesh developed, the hole required for the piezoelectric transducer, and the first barrel grooves with the seal, which is instantaneously formed with the cylindrical part for the FMJ bullet.

### 2.3 Experimental Analysis

The prototypes of the 7.62 mm caseless-coreless ammunitions were manufactured mixing a charge of 2.90 g of double base gunpowder with the binder, moulded into the case shape with the dimensions of a standard ammunition and assembled with the coreless bullet. After that, these were dried in a convection oven at 333.15 °K for 5 h and then the primer of lead styphnate was placed. The coreless bullet is produced in 90/10 brass with a thickness greater than conventional bullets in order to maintain better stability during its flight path. Figure 3 shows the ammunition prototype and the 7.62 mm x 51 mm FMJ ammunition.

Ballistics tests were conducted for 7.62 mm x 51 mm FMJ ammunition under specific international standard<sup>21</sup>. For the experiment of the 7.62 mm caseless-coreless prototype ammunitions, the piston and the firing pin holder were modified to create a hermetic chamber. In both cases, pressure and

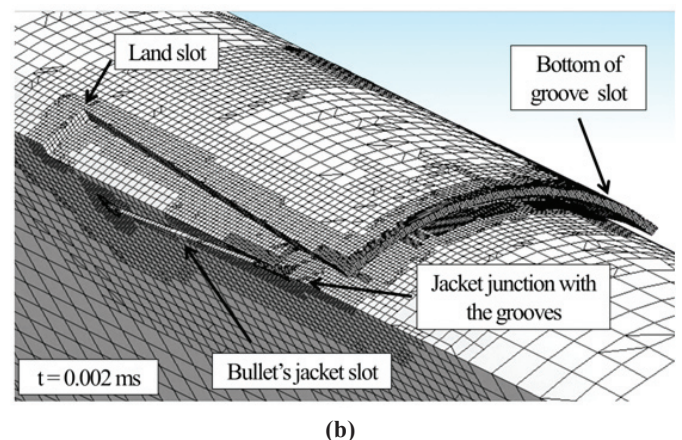
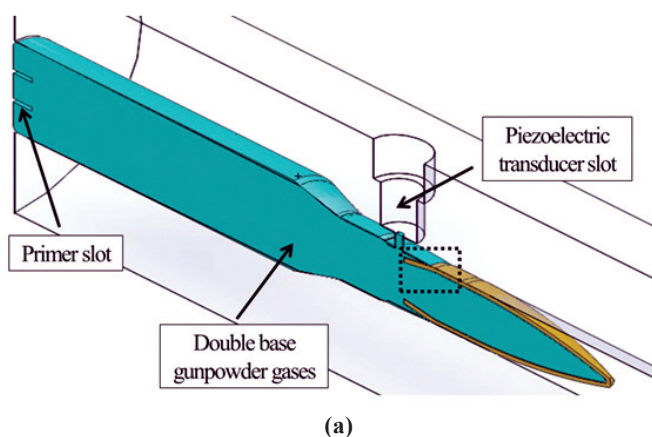


Figure 1. Model of 7.62 mm sealed test barrel chamber (a) with 7.62 mm caseless-coreless ammunition, and (b) close view of the jacket coreless bullet contacting with the grooves.

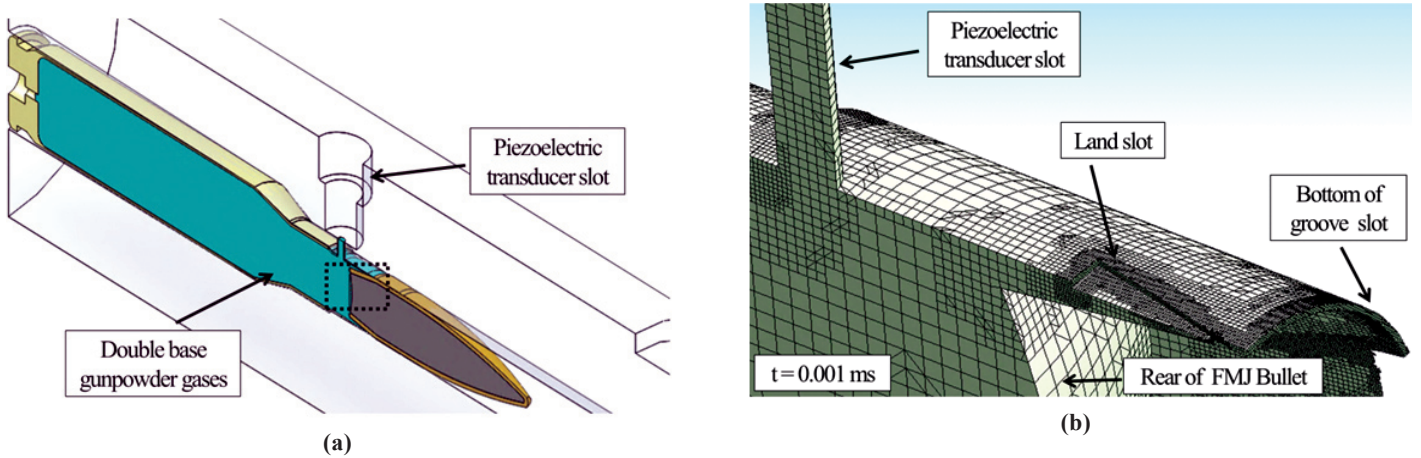


Figure 2. Model of the 7.62 mm test barrel chamber : (a) with FMJ ammunition, and (b) close view of the developed cut-cell mesh.



Figure 3. Ammunitions 7.62 x 51 mm FMJ and 7.62 mm caseless-coreless prototype.

velocity measurements were carried out in 5 series of 10 shots, using a ballistic chronograph and a piezoelectric transducer installed in the chamber of the barrel, as shown in Fig. 4.

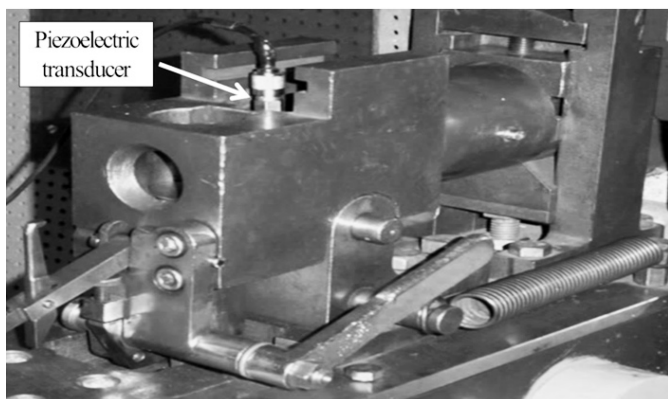


Figure 4. Testing bench with a 7.62 mm x 51 mm barrel.

### 3. RESULTS AND DISCUSSION

The maximum pressure values obtained are shown in Table 1. Pressure measurements were experimentally obtained with a piezoelectric transducer located in the chamber of the barrel. The same volume occupied by the transducer

was included in the FEM model. It was located at the same position to read the pressure value in the numerical analysis. A significant reduction in the maximum pressure of the proposed 7.62 mm ammunition compared to the standard ammunition is observed. That is because the coreless bullet having a lower weight, moves through a longer distance into the barrel. That happens at the beginning of the gunpowder deflagration. Because of that, the combustion chamber expands and the pressure decreases.

Table 1. Maximum pressure in the chamber

Test	7.62 mm caseless-coreless		7.62 x 51 mm FMJ	
	Pressure (MPa)	Time (ms)	Pressure (MPa)	Time (ms)
Numerical	107.66	0.60	272.49	0.27
Experimental	90.00	0.46	273.00	0.30

Table 2 shows the numerical and experimental velocity results for the 7.62 mm caseless-coreless ammunition. These were obtained with a ballistic chronograph that measures experimentally the velocity at an instrumental distance of 23.77 m according to international standards and calculates the velocity of the projectile at the muzzle.

Table 2. Results for 7.62 mm caseless-coreless ammunitions

Test	In the chamber		In the muzzle	
	Pressure (MPa)	Time (ms)	Velocity (m/s)	Time (ms)
Numerical	46.30	2.14	353.92	2.14
Experimental	37.50	2.00	345.00	2.00

The obtained results for the 7.62 mm caseless-coreless ammunition, shows a decrement in the velocity. It can be attributed to a reduction of the pressure in the chamber and the low bullet disinsertion force in comparison with the parameters of the 7.62 x 51 mm FMJ ammunitions, that are shown in Table 3. The 7.62 x 51 mm ammunition has a velocity of 829 m/s – 847 m/s to 23.77 m (ref. 21), so the variation between the experimental and numerical velocities in the muzzle is not

**Table 3. Results for the 7.62 mm x 51 mm FMJ ammunitions**

Test	In the chamber		In the muzzle	
	Pressure (MPa)	Time (ms)	Velocity (m/s)	Time (ms)
Numerical	31.37	1.40	876.65	1.40
Experimental	38.00	1.37	851.00	1.37

considered very wide, which is related to the similarity of their pressure curves.

The pressure distribution caused by the gunpowder deflagration of the 7.62 mm caseless-coreless ammunition is shown in Fig. 5. Pressure variations can be observed by the colour bands, showing that the inner of the bullet without core maintains the same pressure of the last part of the gun barrel. This corresponds to the volume of gases generated at 2.14 ms when the bullet leaves the muzzle barrel. A pressure value of 46.30 MPa in the piezoelectric sensor was obtained, which is close to the experimental value of 37.50 MPa as shown in Table 2.

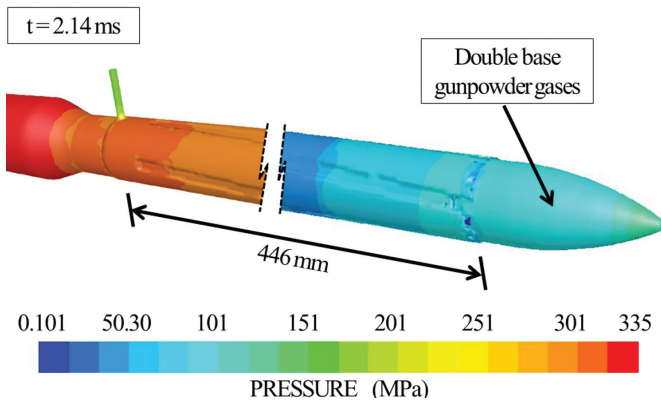


**Figure 5. Pressure distribution for the 7.62 mm caseless-coreless ammunition shot.**

Figure 6 shows the pressure distribution obtained from the stationary system for the shot of the 7.62 mm x 51 mm FMJ ammunition at 1.40 ms. This model corresponds to the internal volume of the barrel. The interior walls and the piezoelectric transducer slot can be observed. The right end includes the geometry formed in the junction of the groove (see Fig. 2) and the bullet's cylinder. Thus, the outlet of the flow gases in this stationary system goes through the bottom of the grooves.

A pressure of 31.37 MPa in the piezoelectric sensor was detected. That matches with the value of 38.00 MPa of the experimental test (shown in Table 3). On the muzzle barrel, the numerical pressure was measured in the bottom side of the grooves, with magnitudes from 10.8 MPa to 92.7 MPa. These correspond to the instant when the bullet leaves the barrel, which cannot be experimentally measured at this location.

A comparison of the pressure curves between the experimental and numerical results for both ammunitions is shown in Fig. 7. The numerical pressure curves were plotted using the results of 10 progressive steady systems and considering smooth lines. When these are compared with experimental curves, these have some variations in their shapes. This is more remarkable in the initial part of the

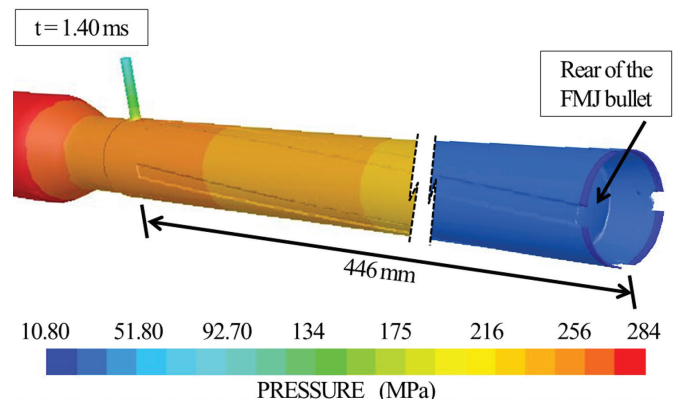


**Figure 6. Pressure distribution for the 7.62 mm x 51 mm FMJ ammunition shot.**

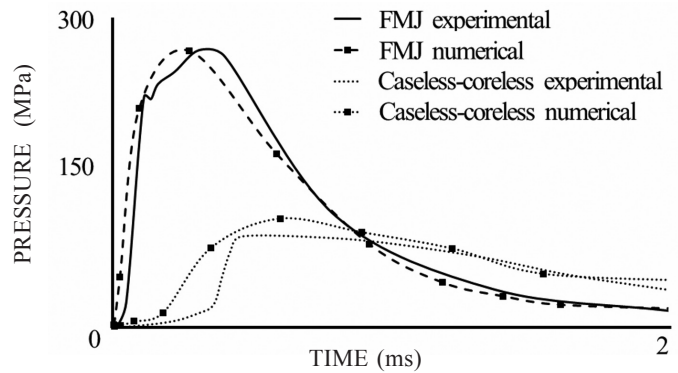


**Figure 7. Pressure curves of 7.62 mm caseless-coreless and 7.62 mm x 51 mm FMJ ammunitions.**

pressure curves for the caseless-coreless ammunition, because the first portion of the graph corresponds to the ignition of the primer and the beginning of the gunpowder deflagration which has a discontinuous behaviour. However, the curves show a progressive form due to the expansion of the chamber combustion. The 7.62 mm x 51 mm FMJ ammunition has a maximum pressure of 270 MPa, and a digressive curve with a continuous decreasing pressure. The 7.62 mm caseless-coreless ammunition has a reduction of its maximum pressure of 90 MPa. This causes a reduction in the resulting velocity and shot range, but remains effective at a distance of 50 m.

**4. CONCLUSIONS**

The internal ballistics of the new designed 7.62 mm caseless-coreless ammunition was carried. Numerical and experimental analyses were conducted on a proposed caseless-coreless prototype ammunition and on a standardised 7.62 mm x 51 mm FMJ ammunition. The shot of the proposed ammunition generates enough power to push the bullet and got similar ballistic parameters to those of the ones produced by the 9 mm x 19 mm FMJ ammunition. It was found that the proposed coreless bullets in caseless ammunition can be used in new weapons intended for short-range combat in urban operations. These can replace commonly used weapons, such as the submachine guns like the 5.7 mm x 28 mm and 9 mm x 19 mm calibres by having the advantage of greater lethality due the aerodynamic shape and size of the 7.62 mm calibre.

The volume of fire can also be increased by the reduction of the weight. Also there is a reduction of the production costs because these ammunitions no longer require a metal case of 70/30 brass.

## REFERENCES

- Chen, J.Y. & Frederick, D. Effects of differential diffusion on predicted autoignition delay times inspired by  $H_2/N_2$  jet flames in a vitiated coflow using the linear eddy model. *Flow Turbul. Combust.*, 2014, **93**, 283–304. doi: 10.1007/s10494-014-9547-3
- Martin, H.T.; Boyer, E. & Kuo, K.K. Effect of initial temperature on the interior ballistics of a 120-mm mortar system. *J. Appl. Mech. T ASME*, 2013, **80**(3), 031408 1-11. doi: 10.1115/1.4023318
- Shekhar, H. Effect of temperature on mechanical properties of solid rocket propellants. *Def. Sci. J.*, 2011, **61**(6), 529-33. doi: 10.14429/dsj.61.774
- Micković, D.; Jaramaz, S.; Elek, P.; Jaramaz, D. & Micković, D. Determination of pressure profiles behind projectiles during interior ballistic cycle. *J. Appl. Mech. T ASME*, 2013, **80**(3), 031402 1-5. doi: 10.1115/1.4023312
- Jaramaz, S.; Micković, D. & Elek, P. Two-phase flows in gun barrel: theoretical and experimental studies. *Int. J. Multiphas. Flow*, 2011, **37**(5), 475–87. doi: 10.1016/j.ijmultiphaseflow.2011.01.003
- Wright, Y.M.; Margari, O.; Boulouchos, K.; De Paola, G. & Mastorakos, E. Experiments and simulations of n-Heptane spray auto-ignition in a closed combustion chamber at diesel engine conditions. *Flow Turbul. Combust.*, 2010, **84**, 49–78. doi: 10.1007/s10494-009-9224-0
- Sung, H.G.; Jang, J.S. & Roh, T.S. Application of eulerian–lagrangian approach to gas–solid flows in interior ballistics. *J. Appl. Mech. T ASME*, 2013, **80**(3), 031407 1-8. doi: 10.1115/1.4023317
- Balabel, A.; Hegab, A.M.; Nasr, M. & El-Behery, S. Assessment of turbulence modeling for gas flow in two-dimensional convergent–divergent rocket nozzle. *Appl. Math. Model*, 2011, **35**, 3408-22. doi: 10.1016/j.apm.2011.01.013
- El-Askary, W.A.; Balabel, A.; El-Behery, S.M. & Hegab, A. Computations of a compressible turbulent flow in a rocket motor-chamber configuration with symmetric and asymmetric injection. *J. Comput. Model Eng. Sci.*, 2011, **82**(1), 29-54.
- Gorji, S.; Seddighi, M.; Ariyaratne, C.; Vardy, A.E.; O'Donoghue, T.; Pokrajac, D. & He, S. Comparative study of turbulence models in a transient channel flow. *Comput. Fluids*, 2014, **89**, 111-23. doi: 10.1016/j.compfluid.2013.10.037
- Bravo, L.; Voegelé, A. & Trouvé, A. Direct numerical simulation of near-wall combustion in a momentum-driven turbulent boundary layer flow. *In 8th U.S. National Combustion Meet*, University of Utah, Utah, USA, 2013.
- Babkovskaia, N.; Haugen, N.E.L. & Brandenburg, A. A high-order public domain code for direct numerical simulations of turbulent combustion. *J. Comput. Phys.*, 2011, **230**(1), 1-12. doi: 10.1016/j.jcp.2010.08.028
- Di Mare, F.; Knappstein, R. & Baumann, M. Application of LES-quality criteria to internal combustion engine flows. *Computational Fluids*, 2014, **89**, 200-13. doi: 10.1016/j.compfluid.2013.11.003
- Jung, S.Y. & Chung, Y.M. Large-eddy simulation of accelerated turbulent flow in a circular pipe. *Int. J. Heat Fluid Fl.*, 2012, **33**, 1-8. doi: 10.1016/j.ijheatfluidflow.2011.11.005
- Konopka, M.; Meinke, M. & Schröder, W. Large-eddy simulation of supersonic film cooling at finite pressure gradients. *High Perform. Comput. Sci. Eng.*, 2011. doi: 10.1007/978-3-642-23869-7\_26
- Mathew, J. Large Eddy simulation. *Def. Sci. J.*, 2010, **60**(6), 598-605. doi: 10.14429/dsj.60.602
- Tu, J.; Yeoh, G. & Liu, C. Computational fluid dynamics a practical approach. Elsevier, United Kingdom, 2013.
- McGregor, I.A. Telescoped ammunition: A future lightweight compact ammunition? *Can. Army J.*, 2009, **12**(2), 75–81.
- Yang, W.; Li, Y. & Ying, S. Burning characteristics of microcellular combustible objects. *Defence Technology*, 2014. doi: 10.1016/j.dt.2014.03.003
- Hegab, A.M.; Sait, H.H.; Hussain, A. & Said, A.S. Numerical modeling for the combustion of simulated solid rocket motor propellant. *Computational Fluids*, 2014, **89**, 29-37. doi: 10.1016/j.compfluid.2013.10.029
- United States Department of Defense. Cartridge, 7.62 mm: NATO, Ball-M80. MIL-DTL-46931, Picatinny Arsenal, USA. 2010.
- ANSYS Release 14.0. ANSYS Fluent theory guide. ANSYS Inc., Canonsburg, P.A. 15317, USA, 2011. pp. 204–206.

## ACKNOWLEDGEMENTS

The authors gratefully acknowledge the financial support of the Mexican government, the Instituto Politécnico Nacional (SIP-20121014 and SIP-20130729) and the Consejo Nacional de Ciencia y Tecnología.

## CONTRIBUTORS

**Mr U.S. Silva Rivera** conducted ballistics tests and analysed the results; also he developed the caseless-coreless ammunition and contributed in the numerical simulations performed.

**Dr J.M. Sandoval Pineda** defined boundary conditions of numerical analysis, developed the hermetic chamber of the barrel test and participated in the ballistic tests.

**Dr O.Susarrey Huerta** analysed the materials used in the caseless-coreless ammunition, defined the governing equations and he helped in the interpretation of results.

**Dr L.A. Flores Herrera** modelled the numerical system used for caseless-coreless ammunition, validating the system with 7.62 x 51 mm FMJ ammunition; also participated in determining the equations that govern the system.

**Dr P.A. Tamayo Meza** participated in the analysis of the heat capacity of propellant used in the caseless-coreless ammunition and contributed in the analysis of results.